

Journal Article

**Molecular characteristics, association and interfacial properties of Gum Arabic harvested from both *Acacia senegal* and *Acacia seyal***

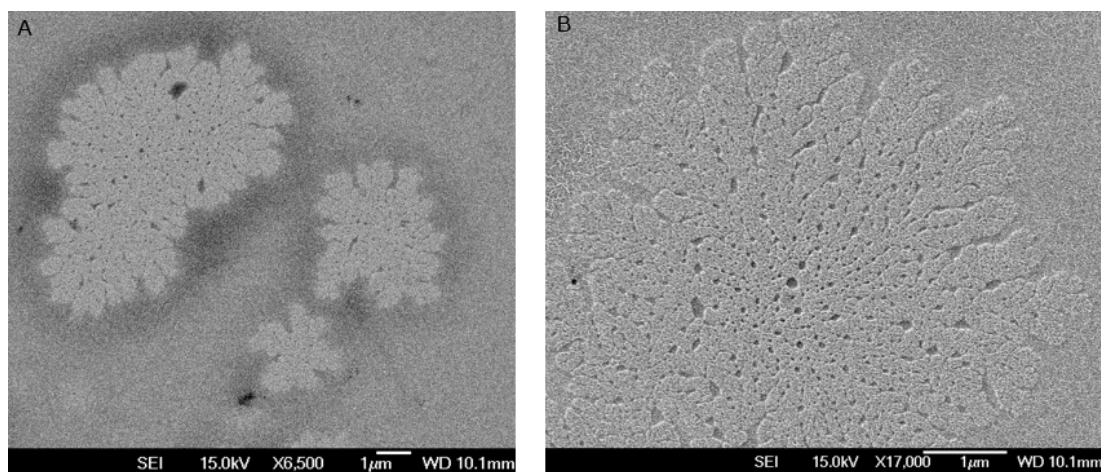
Gashua, I.B., Williams, P.A. and Baldwin, T.C.

This article is published by Elsevier. The definitive version of this article is available at:  
<https://www.sciencedirect.com/science/article/abs/pii/S0268005X16302545>

---

**Recommended citation:**

Gashua, I.B., Williams, P.A. and Baldwin, T. (2016) 'Molecular characteristics, association and interfacial properties of Gum Arabic harvested from both *Acacia Senegal* and *Acacia seyal*', *Food Hydrocolloids*, Dec 2016, vol 61, pp 514-522. doi: [10.1016/j.foodhyd.2016.06.005](https://doi.org/10.1016/j.foodhyd.2016.06.005)



ACCEPTED MANUSCRIPT

1 **Molecular characteristics, association and interfacial properties of Gum Arabic**  
2 **harvested from both *Acacia senegal* and *Acacia seyal*.**

3 **I.B. Gashua<sup>a, b, c</sup>, P.A. Williams<sup>b</sup> and T.C. Baldwin<sup>a, \*</sup>**

4

5 <sup>a</sup> Faculty of Science and Engineering, University of Wolverhampton, Wulfruna St,  
6 Wolverhampton WV1 1LY, U.K.

7 <sup>b</sup> Center for Water Soluble Polymers, Glyndwr University, Plas Coch, Mold Road,  
8 Wrexham, LL11 2AW, U.K.

9 <sup>c</sup> Department of Science Laboratory Technology, Federal Polytechnic Damaturu,  
10 P.M.B 1006, Yobe State, Nigeria.

11

12 \* Corresponding author: Dr T.C. Baldwin, Faculty of Science and Engineering,  
13 University of Wolverhampton, Wulfruna St, Wolverhampton WV1 1LY, U.K.

14 Telephone: +441902 322142

15 Email: [T.Baldwin@wlv.ac.uk](mailto:T.Baldwin@wlv.ac.uk)

16

17

18

19

20

21 **Abstract**

22 The molecular composition of *Acacia senegal* and *Acacia seyal* gum exudate  
23 samples were studied using transmission electron microscopy. The molecules  
24 observed in both samples were found to have diameters of either  $\sim 20\mu\text{m}$ ,  $\sim 60$   
25  $\mu\text{m}$  or  $\sim 10\mu\text{m}$ . These most likely represent the arabinogalactan (AG),  
26 arabinogalactan-protein (AGP) and glycoprotein (GP) molecules present in  
27 *Acacia* gum exudates. Micrographs obtained for gum solutions that had been  
28 left to stand for up to 5 days, indicated that molecular aggregation had  
29 occurred, this was particularly evident for the *Acacia senegal* sample. This  
30 aggregation process was attributed to intermolecular electrostatic interactions.  
31 The adsorbed layer thickness of the gums adsorbed onto polystyrene latex  
32 particles was determined using dynamic light scattering. For the *Acacia senegal*  
33 gum sample, it was found that the adsorbed layer thickness increased over time  
34 and after 14 days had a value of 61nm. These findings are indicative of  
35 multilayer adsorption, through intermolecular electrostatic interaction. For the  
36 *Acacia seyal* gum sample the adsorbed layer thickness was only  $\sim 3\text{nm}$  and did  
37 not increase over time. Transmission electron microscopy revealed the presence  
38 of a distinct, thick adsorbed layer for the *Acacia senegal* gum and the presence  
39 of a much thinner, more diffuse layer for the *Acacia seyal* gum sample.  
40 Emulsification studies showed that the *Acacia senegal* gum was more effective  
41 at stabilising limonene oil-in-water emulsions than the *Acacia seyal* sample and  
42 that this was because markedly more *Acacia senegal* gum adsorbed at the oil-  
43 water interface compared to the *Acacia seyal* gum exudate.

44 **Key words**

45 Gum Arabic, molecular association, adsorbed layer thickness, transmission  
46 electron microscopy.

47

48

49

ACCEPTED MANUSCRIPT

## 50 1. Introduction

51 Gum Arabic is a plant gum exudate obtained from the stems and branches of  
52 specific *Acacia* species, namely *Acacia senegal* and to a lesser extent *Acacia seyal*  
53 which grow across the Sahelian belt of Africa (Williams & Phillips, 2009; Williams,  
54 2012; Williams, Phillips, Stephen, & Churms, 2006). Both of these gums have been  
55 shown to be primarily composed of complex polysaccharides, with a highly  
56 branched structure consisting of galactose, arabinose, rhamnose and glucuronic  
57 acid with the proportions of these varying between the two species (Al-Assaf,  
58 Phillips & Williams, 2005). These gums also contain a small amount of protein,  
59 namely ~2.5% (w/w) in the case of *Acacia senegal* and ~1% (w/w) in the case of  
60 *Acacia seyal*, which is present as an integral part of the structure of the gum.  
61 Recent studies by Lopez-Torrez, Nigen, Williams, Doco and Sanchez, (2015) have  
62 indicated that gum harvested from *Acacia senegal* has a higher degree of branching  
63 than gum harvested from *Acacia seyal*, with more branched galactopyranose  
64 residues, shorter arabinosyl side branches and more terminal rhamnopyranose  
65 residues.

66 The gum obtained from *Acacia senegal* has been shown to consist of three distinct  
67 fractions, which can be isolated by hydrophobic affinity chromatography (Randall,  
68 Phillips, & Williams, 1989; Osman, Williams, Menzies, Phillips, & Baldwin, 1993).  
69 These are referred to as the arabinogalactan (AG), arabinogalactan-protein (AGP)  
70 and glycoprotein (GP) fractions which differ mainly in their molar mass and protein  
71 content (Randall, Phillips, & Williams, 1989; Osman, Williams, Menzies, Phillips, &

72 Baldwin, 1993; Renard, Lavenant-Gourgeon, Ralet, & Sanchez, 2006). The AG  
73 component constitutes ~90% (w/w) of the total gum and has been reported to have  
74 a molar mass and hydrodynamic radius,  $R_h$ , of  $\sim 2.5 \times 10^5$  g/mol, and  $\sim 15$ nm  
75 respectively and it contains very little protein (<1% w/w) (Randall, Phillips, &  
76 Williams, 1988; Osman, Williams, Menzies, Phillips, & Baldwin, 1993). Work by  
77 Sanchez using transmission electron microscopy and atomic force microscopy has  
78 shown that the AG fraction consists of oblate ellipsoids with a  $\sim 20$  nm diameter  
79 and a  $\sim 1.5$  nm thickness with an inner, interspersed chain network (Sanchez,  
80 Schmitt, Kolodziejczyk, Lapp, Gaillard, & Renard, 2008).

81 Arabinogalactan – protein(s) accounts for ~10% (w/w) of the total gum and has a  
82 molar mass and  $R_h$  of  $1-2 \times 10^6$  g/mol and  $\sim 23$ nm respectively and contains ~10%  
83 protein (Randall, Phillips & Williams, 1988; Osman, Williams, Menzies, Phillips, &  
84 Baldwin, 1993; Qi, Fong, & Lamport, 1991; Renard, Garnier, Lapp, Schmitt, &  
85 Sanchez, 2012). This fraction can be degraded by proteolytic enzyme (Mahendran  
86 Williams, Phillips, Al-Assaf, & Baldwin, 2008; Renard, Lepvrier, Garnier, Roblin,  
87 Nigen, & Sanchez, 2014) and hence it has been suggested that the molecules which  
88 constitute this fraction display a “wattle blossom-like” structure with carbohydrate  
89 blocks attached to a polypeptide chain/core protein, as is thought to be typical for  
90 AGPs in general (Fincher, Stone, & Clark, 1983; Randall, Phillips, & Williams, 1989;  
91 Showalter, 2001). Studies by Mahendran have identified carbohydrate blocks of  
92  $\sim 4.5 \times 10^4$  Da linked by O-serine and O-hydroxyproline to a polypeptide chain of  
93 approximately 250 amino acids in length ( $\sim 30$  kDa core protein) present in the AGP  
94 fraction. (Mahendran Williams, Phillips, Al-Assaf, & Baldwin, 2008). More recently,

95 Renard (2012) reported that the AGP present in the gum when in solution adopted  
96 two types of conformation, with two different molecular weights. The low  
97 molecular weight population, with long-chain branching had a compact structure  
98 while the high molecular weight population with a short chain branching had a  
99 more elongated conformation (aggregates of the smaller molecules). Transmission  
100 electron microscopy indicated the presence of two populations of disk – like  
101 molecules with thicknesses below 3-5nm and approximately 85% of the particles  
102 observed displayed an apparent diameter of 20 – 80nm. Small angle neutron  
103 scattering gave a maximum dimension for AGP of 64nm. Single molecules with a  
104 spheroidal shape and aggregated molecules with an elongated shape were both  
105 reported to possess an outer structure combined with an inner porous network of  
106 interspersed chains or interacting blocks (Renard, Garnier, Lapp, Schmitt, &  
107 Sanchez, 2012).

108 The GP fraction constitutes only ~1% of the total gum, has a molar mass of  $2.5 \times 10^5$   
109 and contains up to 50% protein. This fraction is not degraded by proteolytic  
110 enzyme. Studies of the morphology of the molecular components of this fraction  
111 have indicated that when in solution it too contains a mixture of single and  
112 aggregated molecules. These molecules displayed a high propensity to self-  
113 associate in to either linear or circular ring structures. The structure of the single  
114 molecules was that of a thick shell wrapped around a central hole and gave rise to a  
115 ring-like morphology with ~8 – 11 nm diameter (Renard, Lepvrier, Garnier, Roblin,  
116 Nigen, & Sanchez, 2014).



117 However, markedly less attention has been paid to the molecular characteristics  
118 and composition of gum Arabic obtained from *Acacia seyal*. It is known to have a  
119 significantly higher average molar mass than that obtained from *Acacia senegal*,  
120 but interestingly it has a lower intrinsic viscosity indicating a much more tightly  
121 packed structure (Al-Assaf, Phillips, & Williams, 2005; Gashua, Williams, Yadav, &  
122 Baldwin, 2015). Gel Permeation Chromatography studies have shown that this gum  
123 is also polydisperse and that the proteinaceous components are distributed across  
124 the range of molar mass species present (Al-Assaf, Phillips, & Williams, 2005;  
125 Gashua, Williams, Yadav, & Baldwin, 2015).

126 Gum Arabic is widely used in the Food Industry as an emulsifier to stabilise flavour  
127 oil-in-water emulsions for application in beverages (Williams & Phillips, 2009). It has  
128 been proposed that the protein present within the structure of the gum molecules  
129 facilitates their adsorption onto the surface of the oil droplets with the  
130 carbohydrate component protruding into the aqueous phase providing an  
131 electrosteric barrier preventing droplet flocculation and coalescence (Padala,  
132 Williams, & Phillips, 2009). Whilst the gum obtained from *Acacia senegal* is very  
133 effective at forming oil-in-water emulsions this is not the case for that harvested  
134 from *Acacia seyal* (Flindt, Al-Assaf, Phillips, & Williams, 2005).

135 Therefore, the objective of the current study was to gain a clearer understanding of  
136 the mechanisms underlying the differences in the emulsification properties  
137 exhibited by gums obtained from trees of *A. senegal* and *A. seyal*. For this  
138 investigation, we chose to use polystyrene latex particles as a model system to  
139 determine the adsorbed layer thickness, which was studied using a combination of

140 dynamic light scattering and transmission electron microscopy. In addition to which,  
141 the molecular composition and self-assembly of the molecules present in the two  
142 gum samples was investigated by transmission electron microscopy and scanning  
143 transmission electron microscopy.

144

## 145 **2. Materials and methods**

### 146 *2.1. Materials*

147 The samples of *Acacia senegal* and *Acacia seyal* gum exudates used in this study  
148 have been previously described and characterised (Gashua, Williams, Yadav &  
149 Baldwin, 2015) and a summary of their chemical and physicochemical characteristics  
150 are presented in Table 1.

151

152 Polystyrene latex particles of 0.1 $\mu$ m mean particle size were purchased from Sigma-  
153 Aldrich Chemie GmbH, Germany and were in the form of a 10% aqueous dispersion.  
154 The bovine serum albumin (BSA) was obtained from Sigma Aldrich, Gillingham, UK.  
155 Sodium nitrate (analytical grade) and D-Limonene reagents were obtained from  
156 Fisher Scientific, UK. The density of the D-limonene was 0.843g/cm<sup>3</sup>.

157

### 158 *2.2. Methods*

#### 159 *2.2.1. Molecular size*

160 2.2.1.1. *Dynamic light scattering*

161 The hydrodynamic size of the *Acacia senegal* and *Acacia seyal* gum samples and BSA  
162 were determined by dynamic light scattering (Zetasizer, Nano series, Malvern  
163 Instruments). Powdered samples were dissolved in standard deionized water to give  
164 solutions with a concentration of 0.05% w/w. These were filtered using a 0.45µm  
165 pore size filter in order to remove extraneous materials before immediately  
166 transferring 1.5 mL of each into a DTS0012 disposable cuvette and placing them into  
167 the measuring chamber of the instrument. All measurements were performed at  
168 room temperature (25<sup>0</sup>C) and the values reported are the average of 10 subruns.

169

170 *Transmission electron microscopy (negative staining for molecular size and*  
171 *aggregation experiments)*

172 A 1% (w/w) solution of the *A. senegal* and *A. seyal* gum samples were prepared in  
173 sterile deionised water.

174 Formvar/carbon-coated nickel (TEM) grids (200 mesh) were incubated on the  
175 surface of 30 µl drops of the sample solutions for 90 seconds. Excess liquid was  
176 carefully removed by touching the edge of the grids on to filter paper (wick).

177 The grids were then negatively stained by placement on a 30 µl drop of 2% (w/v)  
178 Uranyl acetate for 90 seconds. Excess Uranyl acetate was removed from the grids as  
179 described above. The negatively stained grids were then air dried, prior to being  
180 observed on a JEOL JEM-1200 EX Transmission Electron Microscope, at an

181 accelerating voltage of 80 kV. The images were photographed using a GATAN  
182 retractable multi scan camera.

183

184 *Scanning transmission electron microscopy (for aggregation experiments)*

185 Scanning transmission electron microscopy (STEM) imaging was performed in a  
186 JEOL 7000F SEM using the transmitted electron detector. The work was performed  
187 at 20 kV.

188 Samples were prepared as described previously on formvar/carbon-coated Nickel  
189 200 mesh grids.

190

191 *2.2.2. Adsorbed layer characteristics*

192 *2.2.2.1. Dynamic light scattering*

193 The thickness of the gum Arabic layer adsorbed onto the polystyrene latex particles  
194 was determined by dynamic light scattering using the Malvern Zeta Nano ZS  
195 (Malvern, UK). 9.5 mL of gum Arabic or BSA solutions at concentrations of 0.01 –  
196 0.05% in water and in presence of 0.5M NaNO<sub>3</sub> were added to 0.5 mL of a 0.5%  
197 polystyrene latex dispersion. For the dynamic light scattering measurements, sample  
198 times and delay times were chosen automatically by the instrument software and  
199 analysed by cumulant analysis. Consistent values for the diffusion coefficient were  
200 found from multiple ten sub-run repeats and the particle size calculated. The  
201 hydrodynamic radius of the particles with (  $R_{h,polymer}$  ) and without (  $R_h$  ) polymer

202 adsorbed was determined and the adsorbed layer thickness,  $\delta$ , was calculated  
203 using equation (1)

$$204 \quad \delta = R_{h,\text{polymer}} - R_h \quad (1)$$

205

206

207 *2.2.3. Transmission electron microscopy (negative staining for measurement of*  
208 *adsorbed layer thickness)*

209 The nature of the adsorbed layer for the two gum Arabic samples on polystyrene  
210 latex particles was further investigated by transmission electron microscopy. 9.5 mL  
211 of the *A. senegal* and *A. seyal* solutions at a concentration of 1% in water were  
212 added to 0.5 mL of a 0.5% polystyrene latex dispersion.

213 Formvar coated nickel TEM grids were washed in 30 $\mu$ l of tris buffer saline (1xTBS)  
214 by placement on a drop of the TBS on the surface of a sheet of dental modelling  
215 wax, for 5 minutes. The grids were rinsed with sterile deionized water (SDW) by  
216 floatation on a 30 $\mu$ l drop of SDW for 5 minutes and were then incubated on the  
217 surface of 30 $\mu$ l drops of the sample solutions for 90 seconds. Subsequently the  
218 grids were rinsed with deionized water as described previously, and excess liquid  
219 was carefully removed by touching the edge of the grids on to filter paper.

220 The grids were then negatively stained by placement on a 30 $\mu$ l drop of 2% (w/v)  
221 Uranyl acetate for 90 seconds. Excess Uranyl acetate was removed as described  
222 above. The negatively stained grids were air dried, prior to being observed on a

223 JEOL JEM-1200 EX Transmission Electron Microscope, at an accelerating voltage of  
224 80Kv. The images were photographed using a GATAN retractable multi scan  
225 camera.

226

#### 227 2.2.4. Emulsification properties

228 20%w/w limonene oil-in-water emulsions were prepared according to the method  
229 described by Padala, et al., (2009). 32g of 0.5% (w/w) gum Arabic (*A. senegal* and *A.*  
230 *seyal*) in water was accurately weighed into a container followed by the addition of  
231 8g of D-limonene. The system was sheared using an Ultra Turrax T25 mixer (IKA  
232 Werke GmbH and co DE) equipped with a S25 N18 G rotor set at maximum 24,000  
233 rpm for 4 minutes at a temperature of 25°C.

234 The droplet size and mean specific surface area of the gum Arabic oil-in-water  
235 emulsions was determined by laser diffraction using the Mastersizer 2000 (Malvern  
236 Instruments). The dispersion unit of the instrument was first cleaned with distilled  
237 water while simultaneously varying the agitation speed until the laser intensity  
238 display was about 80%. The emulsion was then added to the water in the dispersion  
239 unit dropwise using a pipette, until the obscuration was between 10-15%. All  
240 measurements were carried out in triplicate and at room temperature and the  
241 average value taken.

242 The prepared emulsions were left to equilibrate for 72 hours before centrifugation,  
243 the supernatant was collected and the molecular mass distribution then determined  
244 by Gel Permeation Chromatography using a Superose 6 column as described

245 previously (Padala, Williams, & Phillips, 2009). The difference in the RI peak areas  
246 before and after emulsification was obtained using the Astra software 4.2.0 and the  
247 amount of gum Arabic adsorbed onto the oil droplets was calculated.

248

### 249 **3.0. Results and discussion**

250

#### 251 *3.1. Molecular size and aggregation of molecules over time*

252 The hydrodynamic radii of the biopolymer samples obtained by dynamic light  
253 scattering are presented in Table 2. The results for both the *Acacia* gums are in  
254 close agreement to the values reported previously (Gashua, Williams, Yadav, &  
255 Baldwin, 2015). The value obtained for BSA is also consistent with values reported  
256 in the literature (Robinson & Williams 2002).

257

258 Electron micrographs of the negatively stained *Acacia* gum samples (1% w/w)  
259 obtained by transmission electron microscopy are presented in Figure 1. It can be  
260 observed that both gum samples contain a majority of molecules with a diameter of  
261 ~20 nm which is the size reported for the AG component of *Acacia senegal* gum  
262 (Sanchez, Schmitt, Kolodziejczyk, Lapp, Gaillard, & Renard, 2008). Both of the  
263 samples were also shown to contain a proportion of molecules with a diameter of  
264 ~60 nm which corresponds to the diameter of the AGP molecules present in gum  
265 Arabic (Renard, Garnier, Lapp, Schmitt, & Sanchez, 2012). In addition, a population

266 of much smaller molecules with a diameter of  $\sim 10\text{nm}$  was also observed to be  
267 present which corresponds to the diameter of the GP component of the gum  
268 (Renard, Lepvrier, Garnier, Roblin, Nigen, & Sanchez, 2014).

269

270 We have previously shown by dynamic light scattering that the *Acacia* gum  
271 molecules have a tendency to aggregate in solution and we concluded that this was  
272 due to electrostatic interaction between protein and glucuronic acid residues  
273 present within the gum structure (Gashua, Williams, Yadav, & Baldwin, 2015). In the  
274 present study, the degree of aggregation of the molecules present in both the gum  
275 samples was monitored over a period of time, using transmission electron  
276 microscopy and scanning transmission electron microscopy. The results of which  
277 are presented in Figures 2 and 3; for samples left standing for 1 and 5 days  
278 respectively. Figure 2 shows the molecular structures present in the samples after  
279 1 day and it is observed that aggregates are present in the *A. senegal* sample  
280 (Figure 2 A) with the majority of molecules with a diameter of  $\sim 40\text{ nm}$  as indicated  
281 with the red arrows and larger molecules with a diameter of  $\sim 66\text{ nm}$  shown with  
282 the blue arrows. However, there is no apparent aggregation in the *A. seyal* sample  
283 at this stage (Figure 2 B). Figure 3 shows the samples after leaving the solution to  
284 stand for 5 days. It was observed that distinct, snowflake-like aggregates were  
285 present in the *Acacia senegal* gum sample, which had a diameter of  $\sim 180\text{ nm}$   
286 (Figure 3 A). The *Acacia seyal* gum was also found to contain aggregates, with a  
287 diameter of  $\sim 60\text{ nm}$ , but the molecules were not organised into a snowflake-like  
288 pattern, rather, they seemed to be ellipsoidal in shape (Figure 3 B). These data are



289 consistent with our previous findings, obtained from dynamic light scattering  
290 studies, which showed that the *Acacia senegal* gum sample aggregated to a much  
291 greater extent than the gum obtained from *Acacia seyal*. This is attributed to the  
292 fact that the *Acacia senegal* sample contains more protein and a greater number of  
293 glucuronic acid groups than the *Acacia seyal* sample.

294

295 Scanning transmission electron microscopy was also performed on an *Acacia*  
296 *senegal* gum sample which had been left to stand for 5 days in order to further  
297 elucidate the structure of the aggregates. The micrographs obtained are presented  
298 in Figure 4 and the snowflake-like structure of the aggregated molecules is clearly  
299 visible.

300

### 301 *3.2. Adsorbed layer characteristics*

#### 302 *3.2.1. Adsorbed layer thickness*

303 Initial studies were undertaken to determine the adsorbed layer thickness of BSA  
304 adsorbed onto polystyrene latex particles and the results are presented in Figure 5.  
305 The adsorbed layer thickness values obtained in water were found to be ~3nm and  
306 are similar to values reported by others (Robinson & Williams, 2002). This value is  
307 consistent with the fact that the molecules have a z-average diameter of 6.6nm as  
308 determined by dynamic light scattering. It is recognised that the adsorption of  
309 globular proteins onto hydrophobic surfaces is facilitated through molecular

310 unfolding which exposes the hydrophobic groups within the protein core and  
311 enables them to adsorb onto the particle surface. The adsorbed layer thickness  
312 values obtained in the presence of 0.5M NaNO<sub>3</sub> are much higher than can be  
313 expected and indicate that bridging flocculation has occurred. It is evident that the  
314 protein adsorbed layer thickness is too small to facilitate stabilisation through steric  
315 repulsive forces.

316 The adsorbed layer thickness values of the *Acacia senegal* and *Acacia seyal* gums  
317 adsorbed onto the polystyrene latex particles in water and in the presence of 0.5M  
318 NaNO<sub>3</sub> are shown as a function of the concentration of gum added and after  
319 various equilibration times in Figures 6a-b and 7. Figure 6a shows the adsorbed  
320 layer thickness for *Acacia senegal* gum adsorbed in water. The first point to note is  
321 that the thickness increases as the amount of gum present increases and then  
322 tends to plateau. The increase is due to an increase in the amount of gum adsorbed  
323 at the surface as the gum concentration is increased. The value obtained for the  
324 adsorbed layer thickness in the presence of 0.05% gum (at plateau coverage) on  
325 Day 0 is 21nm which compares to a value of 29.8nm for the z-average  
326 hydrodynamic diameter of the gum molecules determined by dynamic light  
327 scattering. Since the AGP molecules present within gum Arabic are believed to have  
328 a disk or cylinder-like structure with a thickness of below 3-5nm (Renard, Garnier,  
329 Lapp, Schmitt, & Sanchez, 2012) this would indicate that the molecules do not lie  
330 flat on the surface, but must adsorb end-on or else adsorb as multilayers. It is  
331 particularly interesting to note that the adsorbed layer thickness also increases  
332 significantly with time. For example, for the polystyrene latex particles in the

333 presence of 0.05% gum solution the thickness increases from 21nm to 61nm over a  
334 14 day period. This could be due to molecular rearrangements, molecular exchange  
335 or an increase in the amount of gum adsorbed. The additional adsorption could be  
336 either directly onto the PS latex particle surface or perhaps most likely due to  
337 multilayer adsorption. As reported above and in our previous study, *Acacia senegal*  
338 gum alone self associates in solution through electrostatic interactions between  
339 protein and carboxylate moieties within its structure (Gashua Williams, Yadav, &  
340 Baldwin, 2015). We have also previously reported multilayer adsorption to occur  
341 for sugar beet pectin through a similar mechanism (Siew, Williams, Cui, & Wang,  
342 2008).

343 The adsorbed layer thickness for *Acacia senegal* gum in the presence of 0.5M  
344 NaNO<sub>3</sub> is shown in Figure 6b as a function of the concentration of gum and also  
345 after various time periods. Again, we see an increase in the adsorbed layer  
346 thickness as the concentration of gum is increased which then reaches a plateau  
347 value. The values obtained on Day 0 are significantly greater than for samples  
348 prepared in the absence of electrolyte, for example, an adsorbed layer thickness of  
349 44nm was obtained in the presence of 0.05% gum solutions in 0.5M NaNO<sub>3</sub>  
350 compared to 21nm in water. This value is significantly greater than the value we  
351 obtained for the z-average diameter by dynamic light scattering (29.8nm), but could  
352 be accounted for if preferential adsorption of higher molar mass molecules  
353 occurred. We have shown in the current study by TEM and have reported  
354 previously from studies using GPC/MALLS, that the diameter for the high molar  
355 mass species is typically 40-60nm. These findings are also consistent with the

356 dimensions of the AGP reported by Renard and colleagues (Renard, Lavenant-  
357 Gourgeon, Ralet, & Sanchez, 2006) who suggested that the molecules have a  
358 cylinder-like structure with a diameter of  $\sim 60\text{nm}$  and a thickness below  $3\text{-}5\text{nm}$ .  
359 Since the adsorbed layer thickness is  $61\text{nm}$  in the presence of  $0.5\text{M NaNO}_3$  this  
360 indicates that the molecules may adsorb end-on at the surface. Snowden previously  
361 reported that the adsorption capacity for *Acacia senegal* gum adsorbed onto  
362 polystyrene latex particles was  $\sim 1\text{mg m}^{-2}$  in water and that this increased to  $\sim 5\text{mg}$   
363  $\text{m}^{-2}$  for adsorption from electrolyte (Snowden, Phillips, & Williams, 1987). The  
364 increase in the amount adsorbed is explained by the fact that the electrolyte  
365 screens lateral electrostatic interactions between the gum molecules adsorbed at  
366 the surface allowing more to be accommodated. In addition, as the gum adsorbs  
367 there is an increase in the surface charge (Padala, Williams and Phillips, 2009) which  
368 prevents further molecules in solution from adsorbing due to charge repulsions.  
369 This behaviour is typical for polyelectrolytes generally. The fact that the adsorbed  
370 layer thickness does not increase over time, as is the case in water alone, can be  
371 explained by the fact that the electrolyte would also inhibit intermolecular protein-  
372 carboxylate interactions through charge screening and prevent multilayer  
373 adsorption from occurring. This also agrees with the fact that we observed that  
374 association of the *Acacia senegal* gum molecules alone in aqueous solution was  
375 inhibited in the presence of electrolyte solution (Gashua, Williams, Yadav, &  
376 Baldwin, 2015).

377 Figure 7 shows the adsorbed layer thickness for samples prepared with *Acacia seyal*  
378 gum in water and in the presence of  $0.5\text{M NaNO}_3$ . The adsorbed layer thickness is

379 of the order of ~2-3nm in water and ~0.5nm in 0.5M NaNO<sub>3</sub> which is much less than  
380 the average hydrodynamic diameter of the gum molecules of 34.2nm obtained  
381 from dynamic light scattering measurements. If we assume that the AGP molecules  
382 present in this gum have similar disk or cylinder-like molecular characteristics to  
383 those observed in *Acacia senegal* gum, this suggests that the gum molecules in the  
384 *A.seyal* sample lie flat on the surface of the polystyrene latex particles rather than  
385 end-on. *Acacia seyal* has a lower protein content than *Acacia senegal* and the  
386 protein is less accessible as evidenced by the fact that it is not completely  
387 hydrolysed by proteolytic enzyme hence the molecules will have a lower affinity for  
388 the hydrophobic surface (Flindt, Al-Assaf, Phillips, & Williams, 2005). Our results as  
389 described above and in previous studies (Gashua, Williams, Yadav, & Baldwin, 2015)  
390 also indicate that the molecules present in *Acacia seyal* gum do not self associate  
391 in solution to the same extent as those present in gum obtained from *Acacia*  
392 *senegal* .

393 Electron micrographs of the polystyrene latex particles in the presence and absence  
394 of *Acacia senegal* and *Acacia seyal* gums are presented in Figure 8 (a – f). From  
395 Figure 8 (a and b) it can be observed that the particles themselves in the absence of  
396 either of the *Acacia* gum exudates seem to have been stained by the uranyl acetate,  
397 which is probably due to the fact that the stain is cationic in nature. It is also  
398 apparent that the polystyrene latex particles are polydisperse and display a variety  
399 of sizes. Figures 8 c) and d) confirm that the *Acacia senegal* gum molecules have  
400 formed a distinct, thick adsorbed layer surrounding the particles and Figures 8 e)

401 and f) demonstrate that the *Acacia seyal* molecules have formed a much thinner,  
402 more diffuse layer around the particles.

403 The thickness of the adsorbed layer of *A. senegal* gum (Figure 8 c) and d)) is  
404 approximately 15.5nm which is in reasonable agreement with the value of 21nm  
405 recorded on day 1 for a 0.05 % w/w solution in water from the dynamic light  
406 scattering measurements. The difference is most likely due to the fact that the  
407 adsorbed layer observed by TEM using negative staining has been air-dried prior to  
408 imaging and any residual water will be removed once subjected to the high vacuum  
409 present within the entry chamber of the transmission electron microscope. In direct  
410 contrast, there is no such distinct adsorbed layer on the particles incubated in the  
411 presence of *A.seyal* gum, which is also consistent with the fact that the adsorbed  
412 layer thickness values obtained by dynamic light scattering was very small, namely,  
413 ~2-3nm.

414

### 415 3.3. Emulsification properties

416 The droplet size distributions of the emulsions prepared with the *Acacia senegal*  
417 and *Acacia seyal* gum exudates are presented in Figure 9a and 9b respectively. It is  
418 observed that the droplet size for the freshly prepared emulsions is smaller for  
419 *Acacia senegal* than for *Acacia seyal*. In addition, while the droplet size for the  
420 emulsion prepared using the *Acacia senegal* gum remains constant on storing for a  
421 week, the droplet size for the emulsion prepared using *Acacia seyal* increases. This  
422 is as expected, as it is well known that the gum obtained from *Acacia senegal* has

423 superior emulsification properties compared to that harvested from *Acacia seyal*  
424 (Flindt, Al-Assaf, Phillips, & Williams, 2005). The fact that the *Acacia seyal* gum is  
425 able to form emulsions at all, indicates that it must adsorb at the oil-water interface  
426 to some degree. The amount of gum adsorbed onto the emulsion oil droplets was  
427 calculated from the difference in the areas of the GPC RI elution profiles and was  
428 found to be 3.53 mg/m<sup>2</sup> and 0.77 mg/m<sup>2</sup> for *Acacia senegal* and *Acacia seyal*  
429 respectively. The adsorption data points are included on the adsorption isotherms  
430 previously reported for the adsorption of *Acacia senegal* gum onto limonene  
431 droplets (Padala, Williams, & Phillips, 2009) and shows very good agreement with  
432 these earlier findings ( Figure 10) .

433

#### 434 **4. Conclusions**

435 Transmission electron microscopy experiments have confirmed that the gum Arabic  
436 harvested from both *Acacia senegal* and *Acacia seyal* contain spheroidal shaped  
437 molecules, which vary in size. The majority of these molecules have a diameter of  
438 ~20nm, which is consistent with values previously reported for the AG component  
439 of gum Arabic obtained from *A. senegal*. Whilst a smaller proportion have  
440 diameters of ~ 60nm and ~10nm which most likely correspond to the AGP and GP  
441 components known to be present. It was also observed that the molecules tended  
442 to aggregate in solution over time and this was found to occur to a greater extent  
443 for the gum from *Acacia senegal* compared to *Acacia seyal*. This aggregation  
444 process has been attributed to electrostatic interaction between proteinaceous and

445 uronic acid moieties present within the structure of the gums. *Acacia senegal* gum  
446 contains higher levels of both protein and glucuronic acid than *Acacia seyal* gum  
447 which is consistent with the fact that it aggregates to a greater extent.

448 The thickness of the adsorbed layer of *Acacia senegal* gum molecules on the surface  
449 of polystyrene latex particles was found to increase over time and this has been  
450 attributed to the formation of multilayers which occur as a consequence of  
451 electrostatic interaction. This conclusion is supported by the fact that the thickness  
452 did not change over time for experiments undertaken in the presence of electrolyte  
453 which would act to screen electrostatic interactions between the molecules.  
454 Transmission electron microscopy also showed that gum obtained from *Acacia*  
455 *senegal* formed a distinct, thick layer around the polystyrene latex particles. In  
456 contrast, both dynamic light scattering and transmission electron microscopy  
457 showed that the gum from *Acacia seyal* formed a very thin, diffuse layer on the  
458 surface of the polystyrene latex particles and that there was no evidence of  
459 multilayer adsorption.

460 In emulsification studies, the gum from *Acacia senegal* was found to produce  
461 emulsions with a smaller droplet size than for gum from *Acacia seyal*. Furthermore,  
462 the droplet size for emulsions prepared with gum from *Acacia senegal* remained  
463 constant over time while the droplet size increased for emulsions prepared using  
464 gum from *Acacia seyal* indicating that droplet flocculation and/or coalescence had  
465 occurred. This behaviour is believed to be due to the fact that the amount of  
466 *Acacia senegal* gum adsorbed onto the oil droplets was found to be ~five times that



467 for the gum from *Acacia seyal* which is consistent with the adsorbed layer thickness  
468 studies carried out using polystyrene latex particles.

469

470 **Acknowledgements:** Ibrahim B. Gashua would like to express his gratitude to The  
471 Federal Polytechnic Damaturu, and the Tertiary Education Trust Fund, Nigeria,  
472 2011/12 Staff Training Intervention for providing the financial sponsorship to  
473 enable him to perform this research. The authors would also like to express their  
474 thanks to Paul Stanley and staff of the Electron Microscope Centre,  
475 University of Birmingham; for their help and advice and for use of their TEM/STEM  
476 facilities.

477

478

479

480

481

482

483

484

485

486 **References**

- 487 Al-Assaf, S., Phillips, G. O., & Williams, P. A. (2005b). Studies on *Acacia* exudate  
488 gums: part II. Molecular weight comparison of the *Vulgares gummiferae* series of  
489 *Acacia* gums. *Food Hydrocolloids*, **19**, pp. 661–667.
- 490 Baldwin, T.C., McCann, M.C and Roberts, K. (1993) A novel hydroxyproline-deficient  
491 arabinogalactan protein secreted by suspension-cultured cells of *Daucus carota*:  
492 Purification and partial characterization. *Plant Physiol.*, **103**, pp. 1953–1956.
- 493 Fincher, G.B., Stone, B.A. and Clark, A.E. (1991) Arabinogalactan-proteins: structure,  
494 biosynthesis, and functions. *Annual Review Plant Physiol.*, **34**, pp. 47–70.
- 495 Flindt, C., Al-Assaf, S., Phillips, G.O. and Williams, P.O. (2005) Studies of acacia  
496 exudates gums. Part V. Structural features of *Acacia seyal*. *Food Hydrocolloids*, **9**(4),  
497 pp. 687–701.
- 498 Gashua, I.B., Williams, P.A., Yadav, M.P. and Baldwin, T.C. (2015) Characterisation  
499 and molecular association of Nigerian and Sudanese *Acacia* gum exudates. *Food*  
500 *Hydrocolloids*, **51**, pp. 405–413.
- 501 Lopez – Torrez, L., Nigen, M., Williams, P., Doco, T. and Sanchez C. (2015) *Acacia*  
502 *senegal* vs. *Acacia seyal* gums – Part 1: Composition and structure of  
503 hyperbranched plant exudates. *Food Hydrocolloids*, **51**, pp. 41 – 53.
- 504 Mahendran, T., Williams, P.A., Phillips, G.O., Al-Assaf, S. and Baldwin, T.C. (2008)  
505 New insights into the structural characteristics of the arabinogalactan–protein  
506 (AGP) fraction of gum Arabic. *J. Agric. Food Chem.*, **56**, pp. 9269–9276.

- 507 Osman, M.E., Menzies, A.R., Williams, P.A., Phillips, G.O. and Baldwin, T.C. (1993b)  
508 The molecular characterisation of the polysaccharide gum from *Acacia senegal*.  
509 *Carbohydrate Research*, **246**, pp. 303–318.
- 510 Padala, S.R., Williams, P.A. and Phillips, G O. (2009) Adsorption of gum Arabic, egg  
511 white protein, and their mixtures at the oil-water-interface in limonene oil-in-water  
512 emulsions. *J. Agric. Food Chem.*, **57**, pp. 4964–4973.
- 513 Qi, W., Fong, C. and Lamport, D.T.A. (1991) Gum Arabic glycoprotein is a twisted  
514 hairy rope. *Plant Physiol.*, **96**, pp. 848–855.
- 515 Randall, R.C., Phillips, G.O. and Williams, P.A. (1988) The role of the proteinaceous  
516 component on the emulsifying properties of gum Arabic. *Food Hydrocolloids*, **2**, pp.  
517 131–140.
- 518 Randall, R.C., Phillips, G.O. and Williams, P.A. (1989) Fractionation and  
519 characterization of gum from *Acacia senegal*. *Food Hydrocolloids*, **3**(1), pp. 65–76.
- 520 Renard, D., Garnier, C., Lapp, A., Schmitt, C. and Sanchez, C. (2012) Structure of  
521 arabinogalactan-protein from *Acacia* gum: from porous ellipsoids to supramolecular  
522 architectures, *Carbohydrate Polymers*, **90** (1), pp. 322–332.
- 523 Renard, D., Lavenant-Gourgeon, L., Ralet, M.C. and Sanchez, C. (2006) *Acacia*  
524 *senegal* gum: continuum of molecular species differing by their protein to sugar  
525 ratio, molecular weight, and charges. *Biomacromolecules*, **8**, pp. 2637–2649

- 526 Renard, D., Lepvrier, E., Garnier, C., Roblin, P., Nigen, M. and Sanchez, C. (2014)  
527 Structure of glycoproteins from *Acacia* gum: An assembly of ring-like glycoproteins  
528 modules. *Carbohydrate Polymer*, **99**, pp. 736–747.
- 529 Robinson, S. and Williams, P.A. (2002) Inhibition of protein adsorption onto silica by  
530 polyvinylpyrrolidone, *Langmuir*, **18**, pp. 743–749.
- 531 Sanchez, C., Schmitt, C., Kolodziejczyk, E., Lapp, A., Gaillard, C. and Renard, D.  
532 (2008) The *Acacia* gum arabinogalactan fraction is a thin oblate ellipsoid: a new  
533 model based on small-angle neutron scattering and ab initio calculation. *Biophysical*  
534 *Journal*, **94**, pp. 629–639.
- 535 Showalter, A.M. (2001) Arabinogalactan-proteins : structure, expression and  
536 function. *Cell. Mol. Life Sci.*, **58**, pp. 1399-1417.
- 537 Siew, C.K., Williams, P.A., Cui, S.W. and Wang, Q. (2008) Characterization of the  
538 surface-active components of sugar beet pectin and the hydrodynamic thickness of  
539 the adsorbed pectin layer. *J. Agric. Food Chem.*, **56**, pp. 8111–8120.
- 540 Snowden, M.J., Phillips, G.O. and Williams, P.A. (1987) Functional characteristics of  
541 gum Arabic. *Food Hydrocolloids*, **1**(4), pp. 291–300.
- 542 Williams, P. A. (2012) Structural characteristics and functional properties of gum  
543 Arabic. In Kennedy, J.F., Phillips, G.O. and Williams, P.A (eds.), *Gum Arabic* (special  
544 publication No.333). RSC Publishing, Cambridge. pp. 179–187.
- 545 Williams, P.A., & Phillips, G.O. (2009). Gum Arabic. In G.O. Phillips, & P.A. Williams  
546 (Eds.), *Handbook of Hydrocolloids* (p252-273). Cambridge: Woodhead Publishers.

547 Williams, P.A., Phillips, G.O., Stephen, A.M. and Churms, S.C. (2006) Gums and  
548 Mucilages. In Stephen, A.M., Phillips, G.O., and Williams, P.A. (eds.), *Food*  
549 *polysaccharides and their applications*. CRC Press Taylor and Francis Group, FL. pp.  
550 455–60).

ACCEPTED MANUSCRIPT

551

552

553

554

555

556

557

558

559

560

561

562

563

564

|                   | Rha | Ara  | Gal  | GluA | Protein <sup>a</sup> | Protein <sup>b</sup> | Mw x 10 <sup>5</sup> (g/mol) | Mn x 10 <sup>5</sup> (g/mol) | R <sub>g</sub> (nm) | R <sub>h</sub> (nm) |
|-------------------|-----|------|------|------|----------------------|----------------------|------------------------------|------------------------------|---------------------|---------------------|
| <i>A. senegal</i> | 9.2 | 24.9 | 45.3 | 15.5 | 2.93                 | 2.12                 | 4.85                         | 2.77                         | 13.0                | 13.0                |
| <i>A. seyal</i>   | 2.1 | 32.5 | 44.2 | 13.0 | 0.99                 | 0.69                 | 11.4                         | 6.84                         | 24.0                | 17.3                |

Table 1. Sugar, protein composition, Molar mass and hydrodynamic size of *Acacia* gum exudates.

All results expressed as % w/w on a dry weight basis. Rha= Rhamnose, Ara=Arabinose, GluA=Glucuronic Acid, Mw=Molecular weight, R<sub>g</sub>=Radius of gyration, R<sub>h</sub>=Hydrodynamic radius, <sup>a</sup>=by Kjeldhal analysis using a conversion factor of 6.60 as suggested by Anderson, (1986), <sup>b</sup>=From amino acid analysis (Source; Gashua, et al., 2015).

|                      | <i>A. senegal</i> | <i>A. seyal</i> | BSA |
|----------------------|-------------------|-----------------|-----|
| z-average $R_h$ (nm) | 14.9              | 17.1            | 3.3 |

565

566 Table 2. Hydrodynamic radii of the biopolymers

**FIGURE CAPTIONS**

**Figure 1.** Transmission electron micrographs of *Acacia senegal* (A) and *Acacia seyal* (B) gums, negatively stained at day 0. (Scale bar = 0.2 $\mu$ m). Single molecules of varied sizes are observed in both gum samples as indicated by the arrowed letters (a), (b) and (c). The letter (a) indicates molecules of  $\sim$  60nm (putative AGP), and the letter (b) indicates molecules of  $\sim$  20nm (putative AG), while the smaller molecules, are indicated by the letter (c) which represents molecules  $\sim$  10nm (putative GP).

**Figure 2** Transmission electron micrographs of *A. senegal* (A) and *Acacia seyal* (B) gums negatively stained and observed after 1 day. Aggregation is observed to have started to occur in the *A. senegal* sample (A) with a number of  $\sim$  40nm aggregates observed, (as indicated with the arrowed letter (a)) and a larger aggregate of  $\sim$ 66nm (indicated with the arrowed letter (b)). However, there is no apparent aggregation present in the *A. seyal* gum sample at this stage. The scale bar = 0.2  $\mu$ m in both A and B.

**Figure 3.** Transmission electron micrographs of *Acacia senegal* (A) and *Acacia seyal* (B) gums negatively stained and observed after 5 days. Distinct snowflake-like aggregates were observed in the *A. senegal* gum in varied sizes with an average diameter of  $\sim$  184nm (a), with another aggregate of  $\sim$  420nm (b). The *A. seyal* gum also contains aggregates, with an average diameter range of  $\sim$  37nm (a) and  $\sim$  80nm (b), with a larger aggregate of  $\sim$  320nm (c), but the aggregated molecules are not arranged in a snowflake-like manner, rather they seem more ellipsoidal in shape. The scale bar = 0.2  $\mu$ m in both A and B.

**Figure 4.** Scanning transmission electron micrographs of *Acacia senegal* sample after incubation for 5 days at room temperature. Images taken at two magnifications are shown (A) X6, 500 and (B) X17, 000).

**Figure 5.** Adsorbed layer thickness of BSA as a function of concentration in water and in 0.5M NaNO<sub>3</sub>.



**Figure 6a.** Adsorbed layer thickness of *Acacia senegal* gum sample as a function of concentration in water over 14 days period.

**Figure 6b.** Adsorbed layer thickness of *Acacia senegal* gum sample as a function of concentration in 0.5M NaNO<sub>3</sub> over 7 days period.

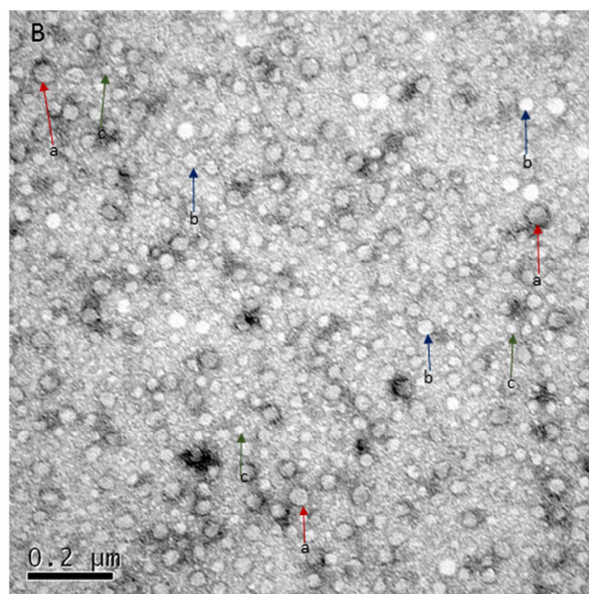
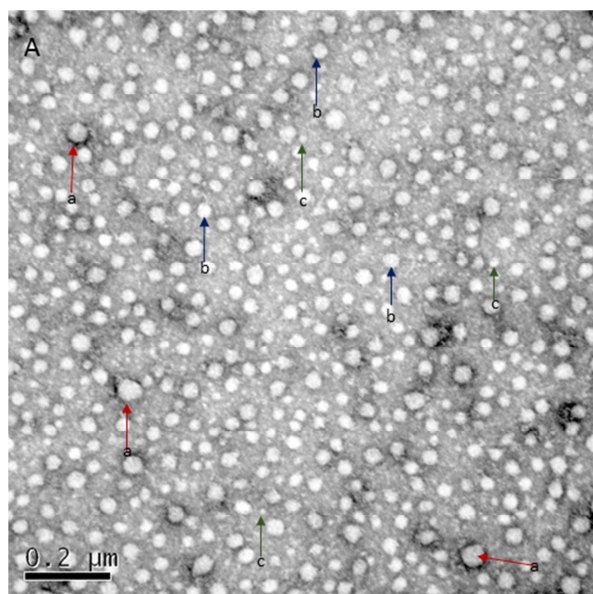
**Figure 7.** Adsorbed layer thickness of *Acacia seyal* gum sample as a function of concentration in water and in 0.5M NaNO<sub>3</sub> over 7 days period. (Where d=day, W=water and S=salt, i.e 0.5M NaNO<sub>3</sub>)

**Figure 8.** (a-b) - TEM Images of Polystyrene latex particles at 100K and 250K magnification; (c-d) TEM Images of Polystyrene latex particles in the presence of *Acacia senegal* gum 100K and 250K magnification. (e-f) - TEM Images of *Acacia seyal* adsorbed onto Polystyrene latex particles at 100K and 250K magnification

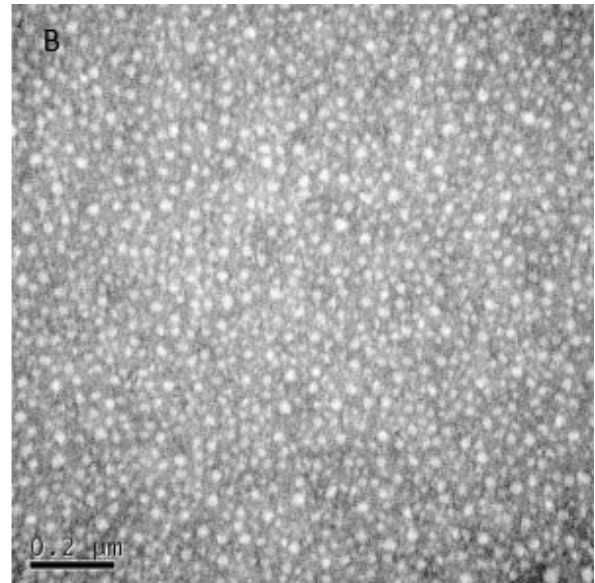
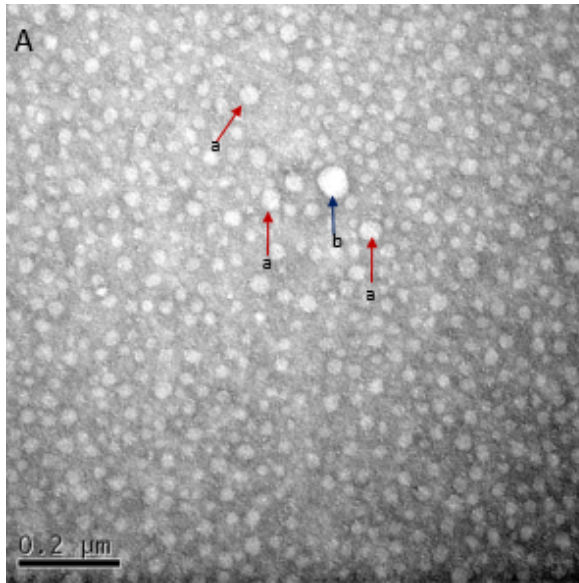
**Figure 9a.** Droplet size distribution of limonene oil-in-water emulsion prepared with *Acacia senegal* stored over 7 days period.

**Figure 9b.** Droplet size distribution of limonene oil-in-water emulsion prepared with *Acacia seyal* stored over 7 days period.

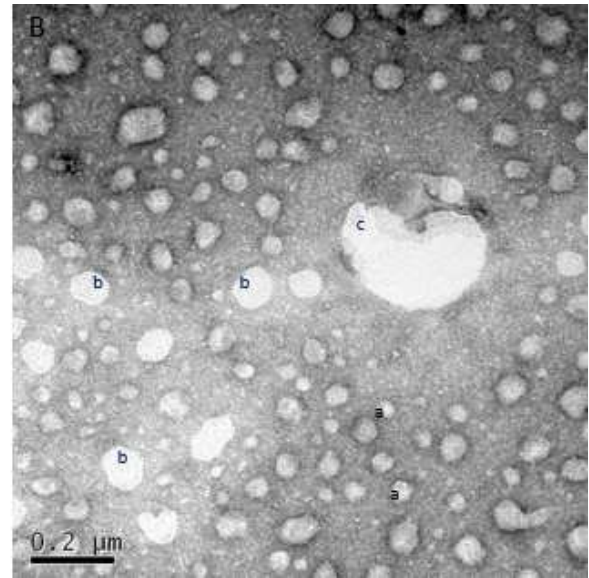
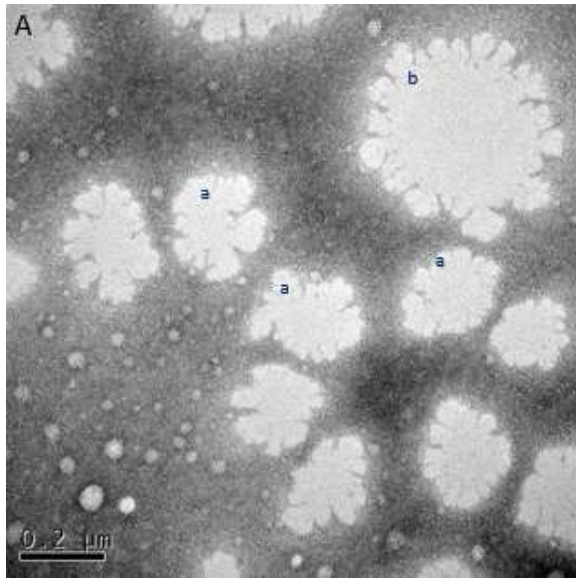
**Figure 10.** Adsorption isotherms for *A. senegal* and *A. seyal* adsorbing onto limonene oil (Adapted from Padala, Williams, & Phillips, (2009). Adsorption of Gum Arabic, Egg White Protein and Their Mixtures at the Oil–Water Interface in Limonene Oil-in-Water Emulsions. Copyright (2009) American Chemical Society.

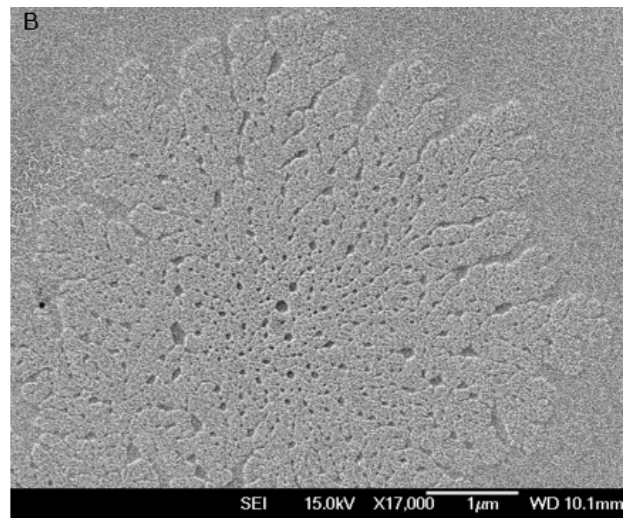
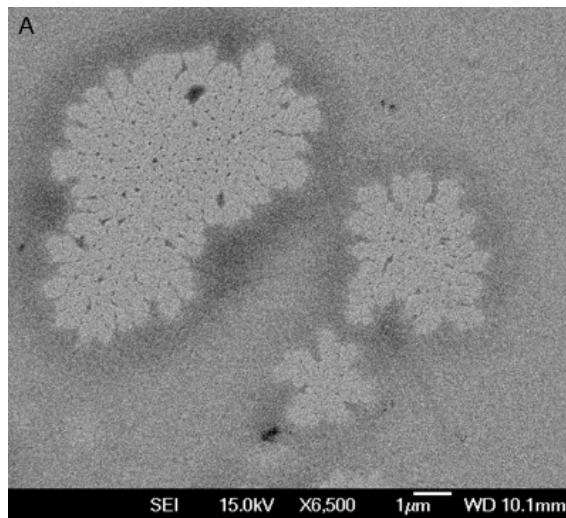


ACCEPTED MANUSCRIPT

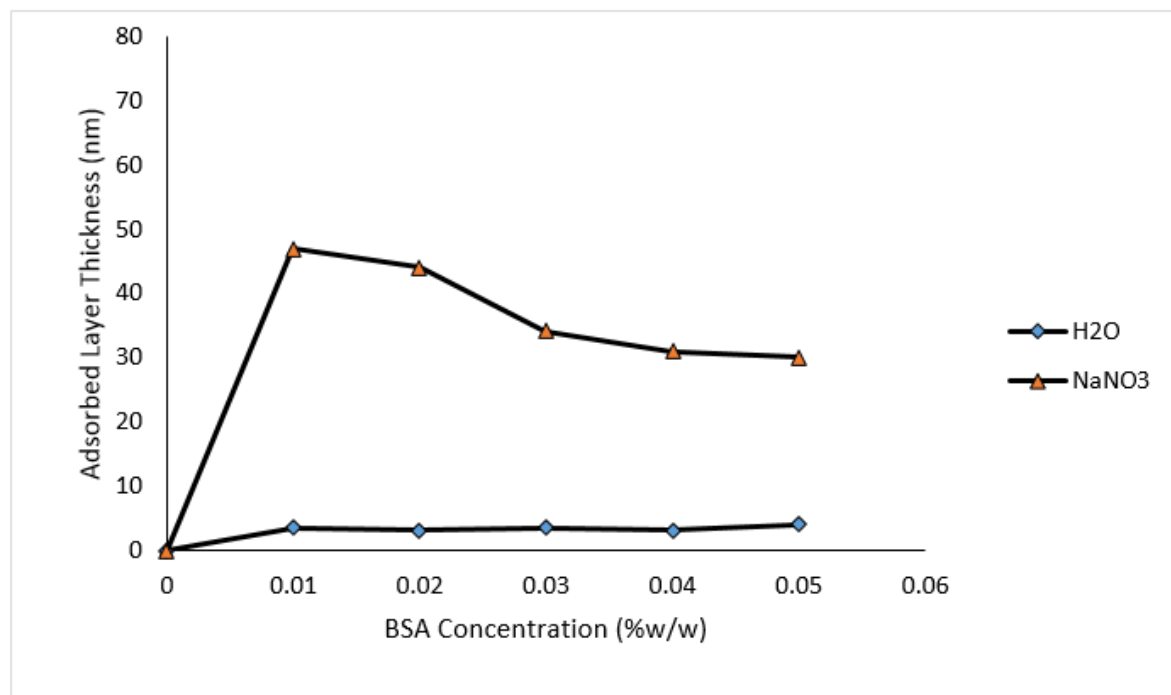


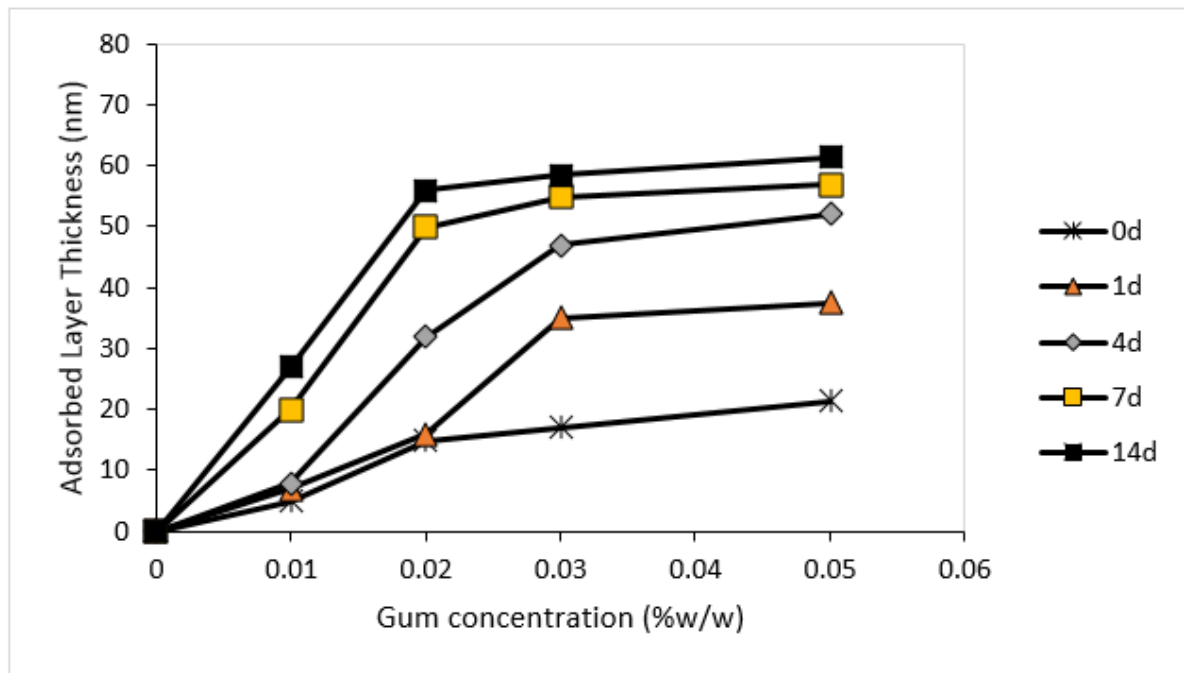
ACCEPTED MANUSCRIPT

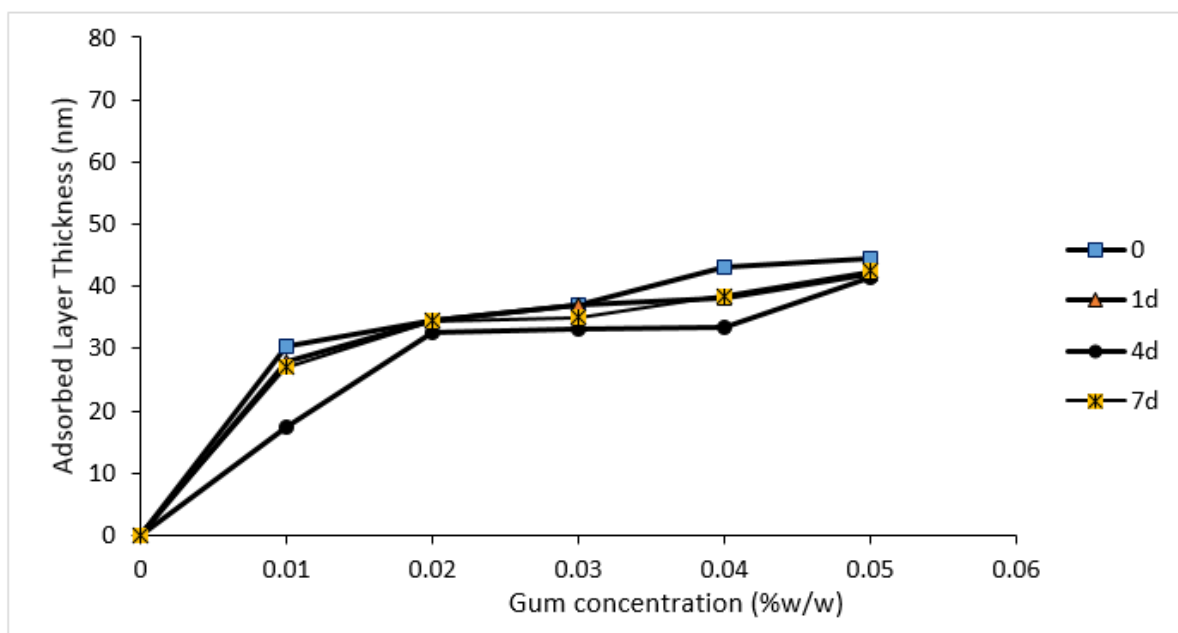




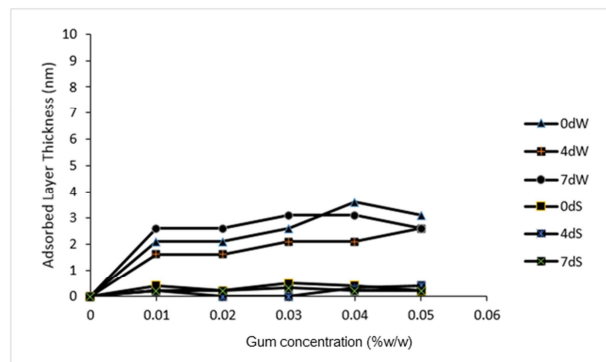
ACCEPTED MANUSCRIPT

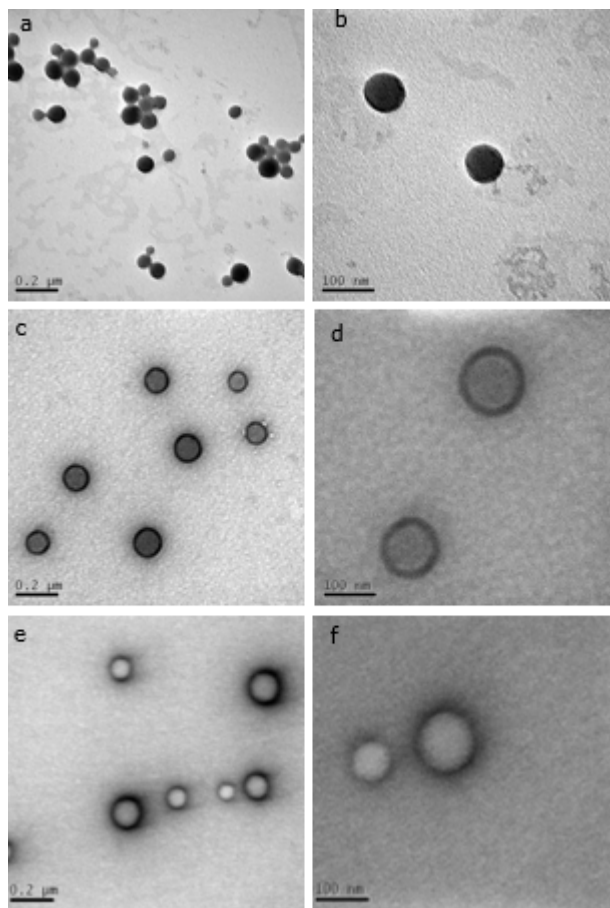


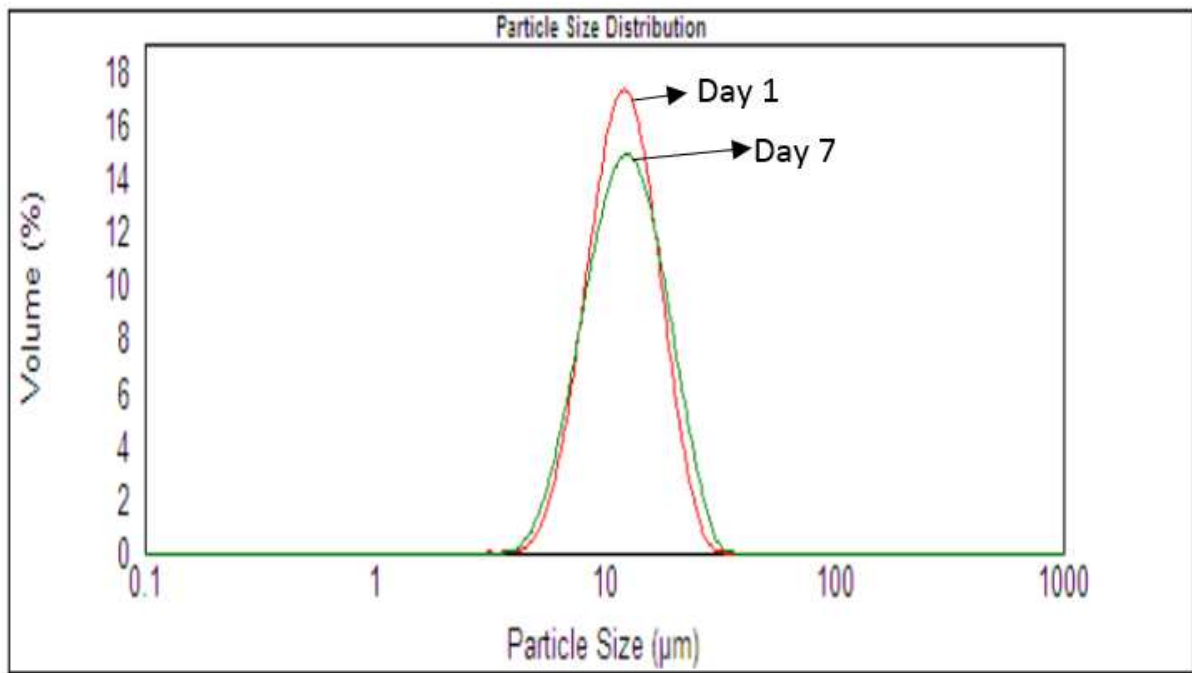




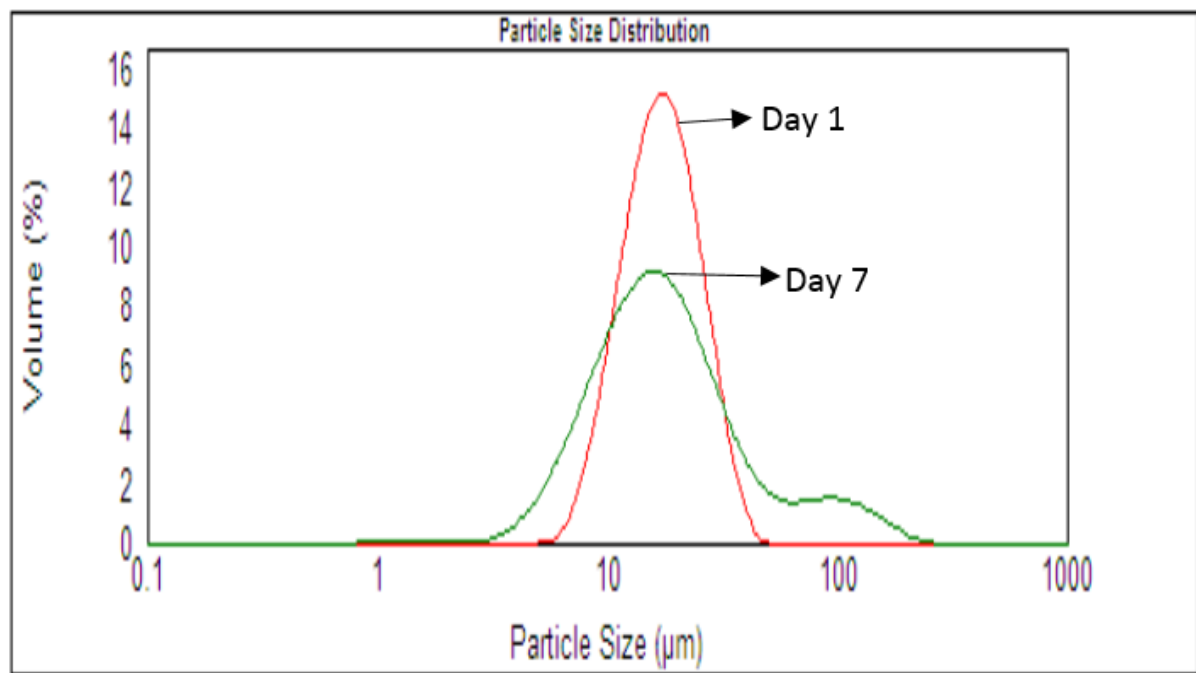


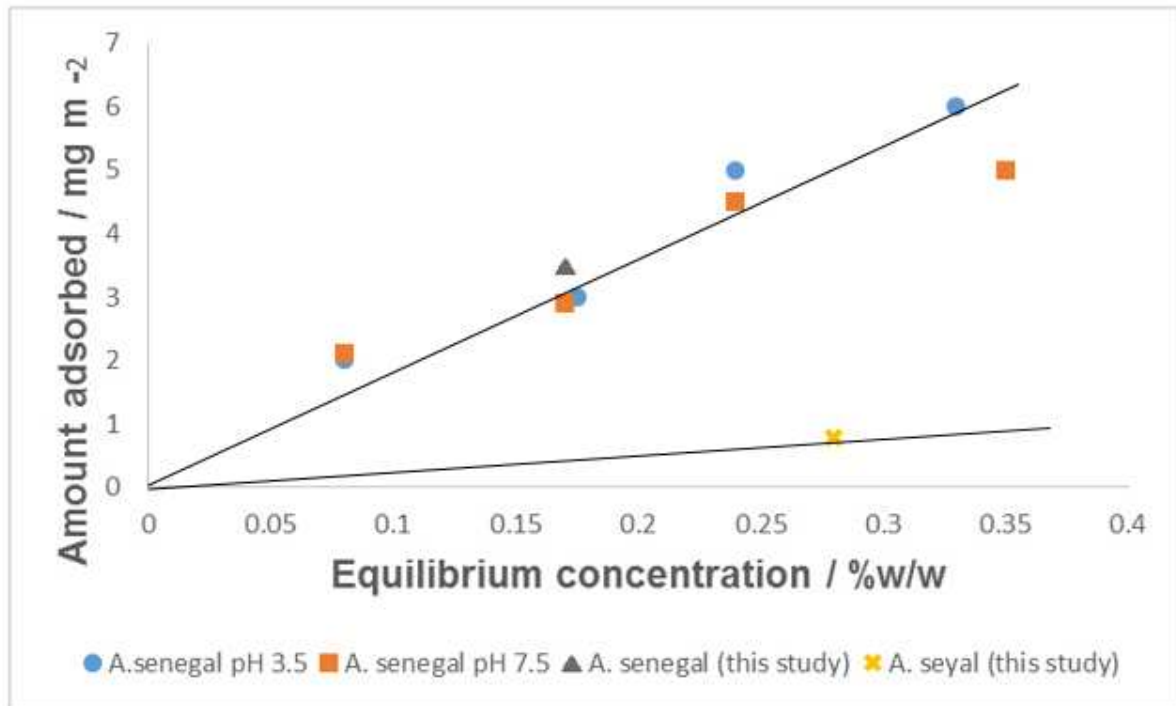






ACCEPTED MANUSCRIPT





## Highlights

- *Acacia* gums in solution display molecular association
- *A. senegal* gum forms multilayers at the solid / liquid interface
- *Acacia* gum composition observed using TEM and STEM.